BIAXIAL VIBRATION ENERGY HARVESTING FOR USE ON AEROSPACE PLATFORMS

Scott D. Moss, Luke A. Vandewater, Joshua E. McLeod, Steve C. Galea
Defence Science and Technology Organisation, Air Vehicles Division,
506 Lorimer Street, Fishermans Bend, 3207, Australia
scott.moss@dsto.defence.gov.au; luke.vandewater@dsto.defence.gov.au;
joshua.mcleod@dsto.defence.gov.au; steve.galea@dsto.defence.gov.au

Keywords: *vibration energy harvesting, scaling, biaxial, electromagnetic, structural health monitoring.*

Abstract

This work describes a vibration harvesting approach that could potentially be used to harvest energy from multi-axial aircraft vibrations. The harvester described is designed to harvest kinetic energy from a vibrating airframe. The harvester uses a wire-coil electro-magnetic (EM) transducer, and a permanent-magnet/ball-bearing oscillator. The bearing moves with two translational degrees of freedom, producing an oscillating magnetic field across the transducer hence generating electrical energy that can be used to power a structural health monitoring sensing device. A prototype harvester has been demonstrated to produce a maximum power of 11.3 mW from a 12 Hz, 300 milli-g host excitation, with a power density of $|P|/L^3 f^2 \sim 3.1\ \mu W/cm^3\ Hz^2$. *The scaling behaviour of a selection of manufactured EM vibration energy harvesters reported in the literature is also examined, and it is determined that harvesters with a scaling length* $L \geq 1.3$ *cm produce the highest power density with an average of* $|P|/L^3 f^2 \sim 11\ \mu W/cm^3\ Hz^2$. *For harvesters with* $L < 1.3$ *cm it is found that the power density rapidly decreases as L is reduced.*

1 Introduction

The Australian Defence Science and Technology Organization (DSTO) is developing a variety of in-situ structural health monitoring (SHM) approaches [1, 2] for potential use in high value platforms across the Australian Defence Force. The SHM systems under development could be employed to: (i) continuously monitor airframe loads and accelerations during flight, (ii) detect damage and damage growth and other structural problems, and (iii) provide a basis for near-real-time damage assessment. The implementation of SHM systems would allow the ADF to move from expensive and time-consuming safety-by-inspection maintenance regimes to more cost-effective automated approaches (in particular the monitoring of airframe fatigue [3] or corrosion [4] 'hot-spots'), and therefore reduce aircraft through-life support costs and increase aircraft availability.

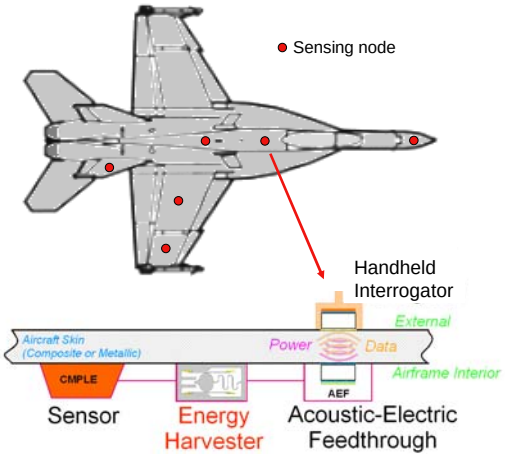

Fig. 1. Schematic of a wireless Structural Health Monitoring system concept with sensing unit, energy harvester and wireless data and power transfer capability.

The DSTO is currently investigating the various components of the generic SHM concept depicted in Fig. 1. The concept involves

three main components, being: (i) a sensor mounted inside the aircraft at a difficult to access location, that is monitoring in-flight mechanical loads on an airframe [5], (ii) with the sensor using energy that is parasitically harvested from local airframe vibrations by an energy harvester [6, 7], and (iii) when the aircraft is on the ground an acoustic electric feedthrough based wireless link is used to download sensor data and to simultaneously provide additional energy to the sensor unit [8, 9]. Energy harvesting is the process of capturing available free energy from the local environment (e.g airframe structural vibrations) and converting it into electrical form [10]. In the context of SHM systems on aircraft, the harvested electrical energy could be used for powering sensor or wireless communications systems.

Energy harvesting approaches for powering SHM systems on air vehicles are being actively explored [11, 12] and trialled [13]. A fundamental issue with many kinetic vibration energy harvesting approaches is that they only harvest vibrational energy from host accelerations along a single-axis (where the host structure may be a location on an airframe). Many single-axis harvesting approaches are described in reference [14]. Recently DSTO has developed a biaxial approach for vibration energy harvesting [15]. Specifically, the approach increases the potential operational directionality from single-axis to 360 degrees in a plane. Host vibrations cause a ball-bearing to oscillate, causing magnetic flux to excite a transducer and hence generate harvestable electrical power.

DSTO is investigating transduction methods for use with the biaxial vibration energy harvesting approach. Previously a magneto-electric transducer was formed using Terfenol-D/piezo-ceramic laminate, (e.g. [16]). This work examines the use of a wire-coil transducer, a schematic of which is shown in Fig. 2, which has also been examined in reference [17]. The bearing shown in Fig. 2 has a diameter of 20 mm, and both the bearing and the host oscillate in the y direction. For experimental and modelling convenience a square magnet geometry was chosen. In this geometry the bearing is free to oscillate in the x - y plane (where x is normal to the page), however, if the host acceleration is aligned with the long (diagonal) edge of the magnet then the bearing oscillates linearly in the y direction. As the bearing oscillates, a region of varying magnetic field passes through the coil inducing a time-varying current, which generates a voltage across an attached electrical load.

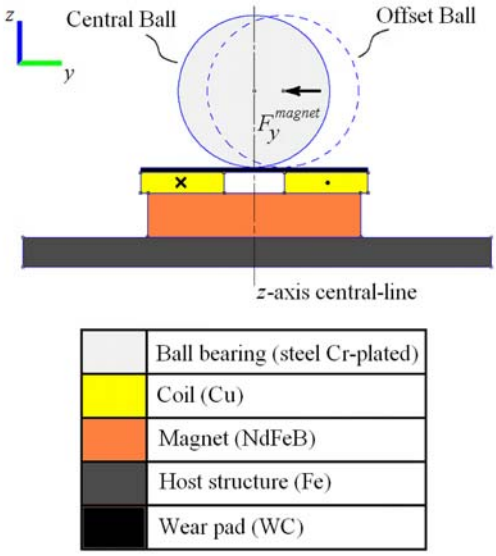

Fig. 2. Schematic of the wire-coil transduction mechanism for the biaxial vibration energy harvester.

One of the benefits of the biaxial harvesting approach (as highlighted in reference [18]) is that it permits a relatively compact design. This paper further explores the important and practical issue of harvester scaling versus output power, in particular the scaling of electro-magnetic vibration energy harvesters and their volumetric power density.

2 Mathematical Analysis

This section will briefly describe the modelling undertaken to predict the steady-state dynamic behaviour of the harvesting arrangement shown in Fig. 2. Equations for the steady state bearing motion and harvested power will be developed.

As reported in reference [16], the restoring force F_y acting between the magnet and the

bearing behaves like a softening spring, of the form,

$$F_y = \alpha\, y + \gamma\, y^3. \quad (1)$$

The spring constants used to model the prototype harvester investigated in this paper are $\alpha = 357$ N/m, and $\gamma = -1.1\times10^6$ N/m^3. As discussed in reference [17], the behaviour of a base-driven mechanical system with a softening spring can be modelled using a forced Duffing equation. If y is the absolute displacement (m) of the bearing and s is the displacement (m) of the host, then the relative motion of the bearing with respect to the base is $u(t) = y(t)-s(t)$. The Duffing equation can be expressed as,

$$\ddot{u}(t) + \frac{\mu}{M}\dot{u}(t) + \frac{\alpha}{M}u(t) + \frac{\gamma}{M}u(t)^3 = -\ddot{s}(t), \quad (2)$$

where the sinusoidal host acceleration is written as,

$$\ddot{s} = a\cos(\Omega t),$$

and where Ω is the host frequency (Hz) and a is the amplitude of the host acceleration (m/s^2), M is the mass of the bearing (kg), $\mu = \mu_M + \mu_E$ is the total damping coefficient (N s/m) with μ_M being the mechanical damping coefficient and μ_E being the electrical damping coefficient, α (N/m) and γ (N/m^3) are spring constants given above.

The displacement of the primary resonance of the nonlinear differential equation (2) can be found using the homotopy analysis method (HAM) as developed by Liao [19]. Substituting $\alpha'=\alpha/M$, $\mu'=\mu/M$ and $\gamma'=\gamma/M$ into equation (2), with $\hbar$ being the auxiliary parameter [20] and β the unknown phase, and solving (2) using HAM yields the relative bearing displacement,

$$u(t) = A_0\cos(\Omega t+\beta) - \frac{\hbar\gamma' A_0^4}{32 M \Omega^2}\cos 3(\Omega t+\beta). \quad (3)$$

A_0 and β and be found by simultaneously solving equations (4),

$$\left\{\left(\alpha' - \Omega^2 + \frac{3\gamma' A_0^2}{4}\right)^2 + \mu'^2\Omega^2\right\}A_0^2 = a^2, \quad (4a)$$

$$\tan\beta = \frac{-4\mu'\Omega}{4(\alpha'-\Omega^2)+3\gamma' A_0^2}. \quad (4b)$$

Since equation (4a) is cubic in A_0^2, there exists either one stable solution, or one unstable and two stable solutions. This leads to multiple branches in the frequency response of the system [21], and hence indicates that the harvester can operate in a high or low energy state within a certain frequency range. In order to determine the electrical power output from the harvester, a well-known generic vibration-to-electricity conversion model is used [22]. The mechanism of the electromagnetic transducer is modelled as a linear viscous damper to the dynamic system, which has been found to accurately represent previously explored linear electromagnetic harvesters [23]. Therefore, the total damping in the mechanical system is a combination of mechanical and electrical damping,

$$\mu = \mu_M + \mu_E. \quad (5)$$

Since the electrical power output is equal to the power removed through electrical damping,

$$P = \int_0^v F dv = \mu_E \int_0^v v dv = \tfrac{1}{2}\mu_E v^2. \quad (6)$$

Finding the derivative with respect to time of solution (3) gives the velocity of the bearing,

$$v(t) = u'(t) = -A_0\Omega\sin(\Omega t+\beta) + \frac{9\hbar\gamma' A_0^4}{32 M \Omega}\sin 3(\Omega t+\beta)\cos^2 3(\Omega t+\beta). \quad (7)$$

Substituting bearing velocity (7) into equation (8) provides a prediction of the harvester's output power,

$$|P| = \tfrac{1}{2}\mu_E |v|^2. \quad (8)$$

Of interest is the power output at the highest energy state possible for the bearing, which is given by the A_0 solution corresponding to the upper branch of equation (4).

3 Experimental

The prototype harvester schematically shown in Fig. 2 was investigated using the experimental arrangement shown schematically in Fig. 3. The chrome-steel ball-bearing (grade AISI 52100) had a diameter of 20 mm, a 30 mm diameter tungsten carbide (6% cobalt by mass, grade KT20) wear-pad with thickness 0.8 mm was used to protect the upper surface of the wound coil and to provide a surface for the bearing to move on. A square NdFeB (grade N42) rare magnet was used and had side length 20 mm and height of 10 mm, with a remanent magnetisation of 1.3 T. Two commercial hard-drive coils (wound from 0.3 mm diameter copper wire) were stacked to create a single 238 turn coil. The coil stack had a height of 4.6 mm, an approximate outer diameter of 30 mm and inner diameter of 10 mm, with a total measured inductance of 4.1 mH and a total measured resistance of 7.5 Ω.

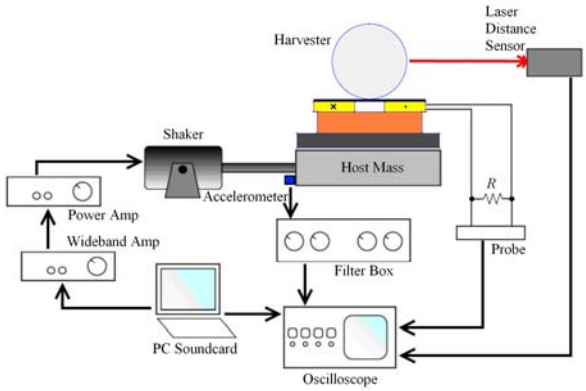

Fig. 3. Experimental arrangement for measuring bearing displacement and coil output across resistive load *R* (drawing not to scale).

As shown in Fig. 3, the bearing displacement was measured using a laser distance sensor. The open circuit ring-down of the bearing displacement was measured to determine the mechanical quality-factor (or Q-factor) of the harvester. A log-decrement approach was used to calculate the damping ratios and hence the Q-factors [24]. Because the magnet/bearing restoring force is nonlinear and softening, the Q-factor used was calculated from the portion of the ring-down curve where the system was considered linear (i.e. for peak bearing y displacements approximately 3 mm or less). The steady state (primary) bearing displacement was measured, with the wire-coil open circuit, for a chosen host acceleration of 300 milli-g (where g = 9.81 m/s^2). The chosen host acceleration level was set near the harvesters centre frequency (15 Hz). The host frequency was then stepped downwards from 20 Hz to 12 Hz in 0.1 Hz steps. The host acceleration reduced to zero and the bearing allowed to come to rest. The chosen host acceleration was then re-applied and the host frequency stepped upwards from 12 Hz to 20 Hz in 0.1 Hz steps. The drive error was approximately ± 20 milli-g rms. Output from the laser distance sensor was recorded using an oscilloscope.

As shown in Fig. 3, a near optimum resistive load R = 7.5 Ω was applied and measurements made of the harvesters output voltage and power. The closed circuit ring-down of the bearing displacement was measured to determine the combined mechanical and electrical quality factor of the harvester. Combined with results from the open circuit ring-down, this allowed estimates to be made of both the mechanical damping coefficient μ_M and the electrical damping coefficient μ_E. A single host acceleration (300 milli-g) was chosen to examine the harvesters steady state electrical output. The chosen host acceleration level was set near the harvesters centre frequency (15 Hz) and the host frequency was swept as described earlier. The harvester's output voltage across the optimised load was recorded using the oscilloscope and probe.

4 Results and Discussion

This section will compare the measured and predicted steady-state bearing displacement and harvester output power, and will then discuss

the scaling of electromagnetic vibration energy harvesters and their volumetric power density.

4.1 Displacement and Power

The mathematical analysis given in Section 2 yielded equation (3) which can be used to examine the steady state (primary) mechanical behaviour of the magnet/bearing system, and equation (8) which can be used to estimate the harvester's output power. In this section predictions from these two equations will be compared with experiment.

As mentioned, the spring constants used to model the prototype harvester are $\alpha = 357$ N/m, and $\gamma = -1.1\times10^{6}$ N/m^3. Measurements of the open-circuit (zero electrical damping) mechanical Q-factor indicated that the mechanical damping coefficient of the harvester was $\mu = \mu_M \sim 0.093$. Using these parameters, equation (3) was used to explore the steady-state (primary) mechanical behaviour of the magnet/bearing system.

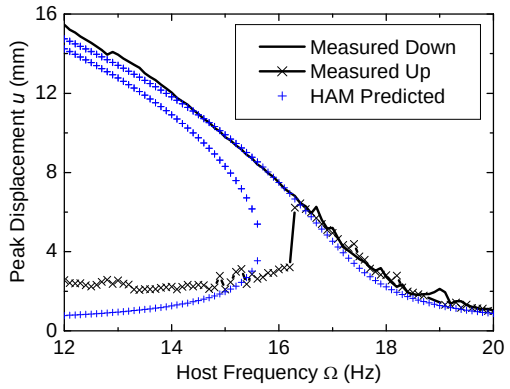

Fig. 4. Measured peak bearing displacement with a base acceleration of 300 milli-g, as a function of frequency and comparison with HAM predictions (where "down" implies a sweep from high to low frequency, and "up" for a sweep from low to high frequency).

Figure 4 plots the predicted bearing displacement against the measured displacement. The predicted displacements are solutions for equation (3) and were found using a host acceleration a = 300 milli-g, and then stepping the host frequency Ω, with the A_0 chosen that corresponds with the solution for the upper branch. The agreement between measured and predicted displacements is reasonable particularly for the uppermost curve corresponding to the measured "down" sweep (where "down" implies that the frequency was stepped from high to low).

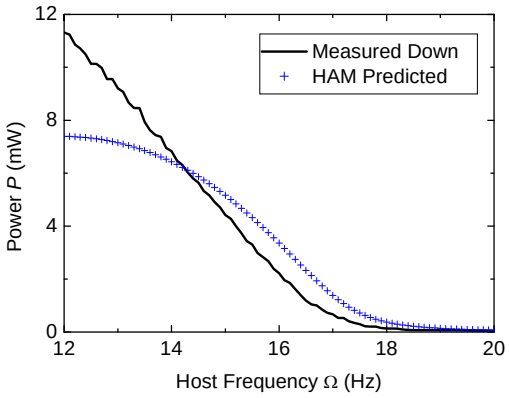

Fig. 5. Measured and predicted harvester output power for a 300 milli-g host acceleration as a function of frequency (where "down" implies a sweep from high to low frequency).

Measurements of the closed-circuit Q-factor, which includes both mechanical and electrical damping, suggested that the combined damping coefficient was $\mu_M + \mu_E \sim 0.106$. The electrical damping coefficient used for modelling was therefore $\mu_E \sim 0.106 - 0.093 = 0.013$. Fig. 5 plots the measured and predicted steady-state harvester output power. Again the agreement between the measured and predicted curves is reasonably good, except in the region between 12 and 14 Hz where the measured output power was greater than predicted. It is believed that non-linearity due to coil asymmetry may have been responsible for the additional measured power. Further work is being carried out to investigate the discrepancy.

Table 1. Power density for oscillatory EM generators (adapted from reference [40]).

Reference	Generator Volume V (cm^3)	Scaling Length $L=V^{1/3}$ (cm)	Vibration Freq. (Hz)	Vibration Accel. (g)	Max. Power (W)	Power Density (W/cm^3)	Power Density Normalised for Freq.$^{-2}$ ($W/cm^3\ Hz^2$)
Yamagucchi U. [25]	123	4.97	2	0.2	1.9E-02	1.5E-04	3.8E-05
U. Tokyo [26]	500	7.94	6	0.4	9.5E-02	1.9E-04	5.3E-06
MIT [27]	23.5	2.86	2	0.3	4.0E-04	1.7E-05	4.3E-06
DSTO [this work]	25	2.92	12	0.3	1.1E-02	4.5E-04	3.1E-06
U. Michigan [28]	2.3	1.32	1		4.0E-06	1.7E-06	1.7E-06
Ferro Solutions [29]	75	4.22	21	0.1	9.3E-03	1.2E-04	2.8E-07
Chinese U. Hong Kong [30]	1	1.00	110	9.7	8.3E-04	8.3E-04	6.9E-08
National Sun Yat-Sen U. [31]	0.45	0.77	60		1.0E-04	2.2E-04	6.2E-08
Perpetuum [32]	130	5.07	100	1.4	4.0E-02	3.1E-04	3.1E-08
U. Southampton [33]	0.24	0.62	322	10	5.3E-04	2.2E-03	2.1E-08
Perpetuum [34]	130	5.07	100	0.1	3.5E-03	2.7E-05	2.7E-09
U. Southampton [35]	0.84	0.94	322	5.4	3.7E-05	4.4E-05	4.3E-10
U. Southampton/Tyndall [36]	0.06	0.39	357	0.4	2.9E-06	4.8E-05	3.7E-10
U. Barcelona [37]	0.6	0.84	360	3.6	2.0E-07	3.3E-07	2.6E-12
U. Sheffield [38]	0.025	0.29	4400	39	3.0E-07	1.2E-05	6.2E-13
Tyndall/U. Southampton [39]	0.1	0.46	1600	0.4	1.0E-07	1.0E-06	3.9E-13
Tyndall/U. Southampton [39]	0.1	0.46	9500	0.4	1.2E-07	1.2E-06	1.3E-14

The agreement shown in Fig. 5 between measured and predicted power suggests that equation (8) provides an adequate description of an EM harvester's output power. In the next section equation (8) will be used to estimate the scaling behaviour of EM harvesters.

4.2 Harvester Scaling

In the previous section it was shown that equation (8) can be used to predict, with adequate accuracy, the output power of the EM harvesting arrangement shown in Fig. 2. Equation (8) will now be used to find a scaling relationship between an EM harvester's output power and device size.

Firstly, a scaling length L is defined where $L \sim V^{1/3}$ and V is the "active" device volume [40]. For example, for the arrangement shown in Fig. 2 the "active volume" is assumed to be the volume the bearing (i.e. the proof-mass [41]) is oscillating in plus the volume of the wire-coil, magnet and wear-pad (totaling ~ 25 cm^3). Assuming that the electrical damping (i.e. damping due to the effect of EM energy harvesting) behaves much like a visco-elastic damper then the electrical damping coefficient scales such that $\mu_E \propto L$ [42]. It is assumed that the host acceleration (and also the harvester's Q-factor) is sufficient to 'ring-up' the steady-state displacement of a harvester's proof-mass to the maximum extent that is physically allowable (i.e. ~L). It is also assumed that a harvester's proof-mass travels approximately length L in one-half of a mechanical cycle (i.e. time $T/2$, where T is the period of the motion). Then $v \propto L/T \propto L f$, where f is the frequency of the resonant motion. The velocity term in equation (8) hence scales as $v^2 \propto L^2 f^2$, and equation (8) scales as,

$$|P| = \tfrac{1}{2}\mu_E |v|^2 \propto L^3 f^2 \qquad (9)$$

or

$$\frac{|P|}{L^3 f^2} \sim k \qquad (10)$$

where k is a constant, i.e. the power density $|P|/L^3 f^2$ is a constant and hence would not be expected to scale with L as long as the assumptions made above are valid. Table 1 is adapted from Arnold [40], and incorporates a selection of manufactured EM generators (or harvesters) found in the literature including both commercial and academic. The harvesters summarised in Table 1 have been ranked according to the right hand column which is the power density calculated using equation (10).

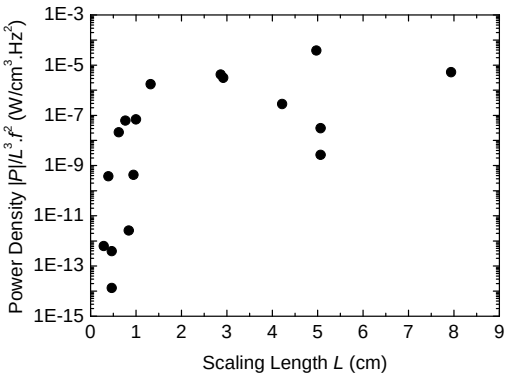

Fig. 6. Harvester power density $|P|/L^3 f^2$ versus scaling length L. Plotted data is taken from Table 1.

The five top ranked harvester designs (all with scaling length $L \geq 1.3$ cm) demonstrate an average power density of $|P|/L^3 f^2 \sim 11$ μW/cm^3 Hz^2, with the best having a maximum of 38 μW/cm^3 Hz^2. Harvester power density $|P|/L^3 f^2$ versus scaling length L is plotted in Figure 6 and shows that the power density is upper bound at ~ 10 μW/cm^3 Hz^2 for harvesters with scaling length $L \geq 1.3$ cm. A designer of EM vibration energy harvesting devices for SHM could use the 10 μW/cm^3 Hz^2 power density figure as a design 'rule-of-thumb'. For harvesters where $L < 1.3$ cm Fig. 6 shows that the power density rapidly decreases as L is reduced. The rapid decrease in power density below $L \sim 1.3$ cm may be due to the increasing dominance of magnetic fringing effects as the scaling length L is reduced.

5 Conclusion

A biaxial energy harvesting approach suitable for use in the aerospace environment has been demonstrated and is capable of producing 11.3 mW from a 12 Hz, 300 milli-g host excitation. The nonlinear Duffing equation (solved using the homotopy analysis method) was found to adequately describe the harvester's mechanical and electrical behaviour. The "active" volume of the non optimised harvester prototype was calculated to be 25 cm^3, and hence the power density of the device was found to be $|P|/L^3 f^2 \sim 3.1$ μW/cm^3 Hz^2. The power densities of a selection of manufactured harvesters reported in the literature were also examined. A scaling length L was defined where $L \sim V^{1/3}$ and V is the "active" harvester volume. It was found that harvesters with a scaling length $L \geq 1.3$ cm have a power density that is upper bound near 10 μW/cm^3 Hz^2, and it is suggested that this power density figure could be used as a design 'rule-of-thumb'. It was also found that the power density of EM harvesters decreases rapidly as L is reduced to less than 1.3 cm.

Acknowledgements

The authors would like to thank Mr. Ian Powlesland for useful discussions regarding power density calculations.

Copyright Statement

References

[1] Galea S, van der Velden S, Moss S, Powlesland I. On the way to autonomy: the wireless-interrogated and self-powered 'Smart Patch' system. *Encyclopedia of Structural Health Monitoring*. 1st Edition, John Wiley & Sons, 2009.

[2] Galea, S C, Powlesland, I G, Moss S D, Konak M, Van der Velden S, Stade B, Baker A A. Development of structural health

monitoring systems for composite bonded repairs on aircraft structures. *Proceedings of SPIE,* Vol. 4327, pp. 246-257, 2001.

[3] Barter S A, Molent L, Wanhill R J H. Typical fatigue-initiating discontinuities in metallic aircraft structures. *International Journal of Fatigue*, Vol. 41, pp. 11-22, 2012.

[4] Hinton B. 2009 Frank Newman Speller award lecture: prevention and control of corrosion in aircraft components - Changes over four decades. *Corrosion*, Vol. 66, No. 8, pp. 0850011-08500115, 2010.

[5] Galea S, Powlesland I. Caribou loads flight survey using a rapid operational loads measurement approach. *Materials Forum*, Vol. 33, p. 100-109, 2009.

[6] Moss S, Powlesland I, Galea S, Carman G. Vibro-impacting power harvester. *Proceedings of SPIE*, Vol. 7643, Art. 76431A, 2010.

[7] Moss S, Barry B, Powlesland I, Galea S, Carman G P, A low profile vibro-impacting power harvester with symmetrical stops. *Applied Physics Letters*, Vol. 97, Art. 234101, 2010.

[8] Moss S, Phoumsavanh C, Konak M, Tsoi K, Rajic N, Galea S, Powlesland I, McMahon P. Design of the acoustic electric feedthrough demonstrator mk-II. *Materials Forum,* Vol. 33, p. 187-200, 2009.

[9] Moss S, Skippen J, Konak M, Powlesland I, Galea S. Detachable acoustic electric feedthrough. *Proceedings of SPIE,* Vol. 7647, Art. 764745, 2010.

[10] Beeby S, White N. *Energy Harvesting for Autonomous Systems*. Artech House Boston, 2010.

[11] Anton S R. *Baseline-free and self-powered structural health monitoring*. Thesis, Virginia Polytechnic Institute and State University, 2008.

[12] Anton S R, Erturk A, Inman D J. Multifunctional unmanned aerial vehicle spar for low-power generation and storage. *Journal of Aircraft*, Vol. 49, pp. 292-301, 2012.

[13] Arms S W, Townsend C P, Churchill D L, Moon S M. Energy Harvesting Wireless Sensors for Helicopter Damage Tracking. *Proc AHS Int. Forum*, Phoenix, U.S.A., Vol. 62, 2006.

[14] Priya S. and Inman D. J., 2009, *Energy Harvesting Technologies*, New York: Springer.

[15] Moss S. Vibration energy conversion device. *U.S. Patent Application* 61/482,496, 2012.

[16] Moss S D, McLeod J E, Galea S C. Wideband vibro-impacting vibration energy harvesting using magnetoelectric transduction. *Journal of Intelligent Material Systems and Structures.* doi: 10.1177/ 1045389X12443598, 2012.

[17] Moss S D, Vandewater L A, Galea S C. Modelling of mechanical nonlinearity in an electromagnetic vibration energy harvester using a forced Duffing equation. *Proc. ASME Conference on Smart Materials, Adaptive Structures and Intelligent Systems*, Stone Mountain, Georgia, USA, SMASIS2012-7910, 2012.

[18] Moss S D, McLeod J E, Powlesland I J, Galea, S C. A bi-axial magnetoelectric vibration energy harvester. *Sensors and Actuators A: Physical*, Vol. 175, No., pp. 165–168, 2012.

[19] Liao S, Tan Y. A General Approach to obtain Series Solutions of Nonlinear Differential Equations. *Studies in Applied Mathematics*, Vol. 119, pp. 297-354, 2007.

[20] Yuan P, Li Y. Approximate Solutions of Primary Resonance for Forced Duffing equation by means of Homotopy Analysis Method. *Chinese Journal of Mechanical Engineering*, Vol. 24, No. 3, pp. 1-6, 2011.

[21] Kovacic I, Brennan, M J. *The Duffing Equation: Nonlinear Oscillators and their behaviour*. Wiley-West Sussex, 2011.

[22] Roundy S, Wright P K, Rabaey M. *Energy scavenging for wireless sensor networks: with special focus on vibrations*. Springer, 2003.

[23] Williams C B, Yates R B. Analysis of a micro-electric generator for Microsystems. *Sensors and Actuators A: Physical*, Vol. 52, No. 8, pp. 8-11, 1996.

[24] Inman D J. *Engineering vibrations*. Upper Saddle, NJ:Pearson Education Inc., 2008.

[25] Nakano K, Saito T, Nakayama A, Kurose T. A portable generator using vibration due to human walking. *Tech. Dig. Int. Workshop Power MEMS (Power MEMS 2002)*, Tsukuba, Japan, pp. 114–117, *2002.*

[26] Sasaki K, Osaki Y, Okazaki J, Hosaka H, Itao K. Vibration based automatic power-generation system. *Microsystems Technology*, Vol. 11, No. 8–10, 2005.

[27] Amirtharajah R, Chandrakasan A P. Self-powered signal processing using vibration-based power generation. *IEEE Journal of. Solid-State Circuits*, Vol. 33, No. 5, pp. 687–695, 1998.

[28] Kulah H, Najafi K. An electromagnetic micro power generator for low-frequency environmental vibrations. *Proc. 17th Int. Conf. MEMS (MEMS 2004)*, Maastricht, The Netherlands, pp. 237–240, 2004.

[29] Ferro Solutions Energy Harvester Data Sheet [Online]. Available: http://www.ferrosi.com .

[30] Ching N N H, Wong H Y, Li W J, Leong P H W, Wen Z. A laser-micromachined multi-modal resonating power transducer for wireless sensing systems. *Sensors and Actuators A*, Vol. 97, pp. 685–690, 2002.

[31] Pan C T, Hwang Y M, Hu H L, Liu H C. Fabrication and analysis of a magnetic self-power microgenerator. *Journal of. Magnetic Material*, Vol. 304, No. 1, pp. e394–e396, 2006.

[32] Perpetuum PMG17-100 Data Sheet [Online]. Available: http://www.perpetuum.co.uk/ .

[33] El-hami M, Glynne-Jones P, White N M, Hill M, Beeby S, James E, Brown A D, Ross J N. Design and fabrication of a new vibration-based electromechanical power generator. *Sensors and Actuators A*, Vol. 92, No. 1–3, pp. 335–342, 2001.

[34] Perpetuum PMG17-100 Data Sheet [Online]. Available: http://www.perpetuum.co.uk/ .

[35] Glynne-Jones P, Tudor M J, Beeby S P, White N M. An electromagnetic, vibration-powered generator for intelligent sensor systems. *Sensors and Actuators A*, Vol. 110, No. 1–3, pp. 344–349, 2004.

[36] Beeby S P, Tudor M J, Torah R N, Roberts S, O'Donnell T, Roy S. Experimental comparison of macro and micro scale electromagnetic vibration powered generators. *Microsystems Technology*, Vol. 13, No. 11–12, pp. 1647–1653, 2007.

[37] Serre C, Pérez-Rodríguez A, Fondevilla N, Morante J R, Montserrat J, and Esteve J. Vibrational energy scavenging with Si technology electromagnetic inertial microgenerators. *Microsystems Technology*, Vol. 13, No. 11–12, pp. 1655–1661, 2007.

[38] Shearwood C, Yates R B. Development of an electromagnetic microgenerator. *Electronics Letters*, Vol. 33, No. 22, pp. 1883–1884, 1997.

[39] Koukharenko E, Beeby S P, Tudor M J, White N M, O'Donnell T, Saha C, Kulkarni S, Roy S. Microelectromechanical systems vibration powered electromagnetic generator for wireless sensor applications. *Microsystems Technology*, Vol. 12, No. 10–11, 2006.

[40] Arnold D P. Review of Microscale Power Generation. *IEEE Transactions on Magnetics*, Vol. 43, No. 11, pp. 3940-3951, 2007.

[41] Kim M, Hoegen M, Dugundji J, Wardle B L. Modelling and Experimental Verification of Proof Mass Effects on Vibration Energy Harvester Performance. *Smart Materials and Structures*, Vol. 19, No. 4, Art. 0405023, 2012.

[42] Drexler K E. *Nanosystems: Molecular Machinery, Manufacturing and Computation*, Wiley:New York, 1992.